American Mineralogist, Volume 91, pages 1425–1431, 2006

Electron paramagnetic resonance spectroscopic study of carbonate-bearing fluorapatite: New defect centers and constraints on the incorporation of carbonate ions in apatites

SERGIY M. NOKHRIN,[1] YUANMING PAN,[1,*] AND MARK J. NILGES[2]

[1]Department of Geological Sciences, University of Saskatchewan, Saskatoon, SK S7N 5E2, Canada
[2]Illinois EPR Research Center, University of Illinois at Urbana-Champaign, Urbana, Illinois

ABSTRACT

X-band electron paramagnetic resonance (EPR) spectra of gamma-irradiated crystals of carbonate-bearing fluorapatite from the Levant mine, Cornwall, England, revealed the presence of two previously characterized centers (i.e., an O^- defect and an $O^-\square_F$ defect, where $\square_F$ represents a vacancy at the F site), a CO_2^- radical, and a new oxygen-associated hole-like center in the anion column. The $O^-\square_F$ center in carbonate-bearing fluorapatite is stable at room temperature, whereas in carbonate-free fluorapatite the stability of this radical is shifted to lower temperatures (<225 K). The CO_2^- radical herewith first reported in carbonate-bearing fluorapatite is characterized by an axial symmetry at room temperature but a weakly orthorhombic symmetry at 77 K, similar to its counterpart in carbonate-bearing hydroxylapatite. This CO_2^- radical most likely formed from Type A carbonate ions by the loss of an O atom and trapping of an electron during gamma irradiation. The single-crystal EPR spectra of the new hole-like center are characterized by the absence of any hyperfine interactions and a strongly orthorhombic symmetry. The spin Hamiltonian parameters of this new center suggest a structural model involving the trapping of a hole by a substitutional oxygen ion sandwiched between two fluorine ion vacancies in the anion column and strongly disturbed by vacancies at the neighboring Ca2 and O3 sites, suggesting a complex substitution of the type: $\square_F O^{2-}\square_F + \square_{Ca2} + CO_3^{2-} \rightarrow F^-F^-F^- + Ca^{2+} + PO_4^{3-}$.

Keywords: EPR spectroscopy, fluorapatite, CO_2^- radical, new O^- center, carbonate ions

INTRODUCTION

Carbonate-bearing fluorapatite and hydroxylapatite are major constituents of phosphorite deposits and are major mineral components of mineralized tissues (bones, teeth, and fossils) of amphibians, reptiles, and mammals. Consequently, carbonate-bearing apatites have attracted active research from not only mineralogists and geochemists but also scientists among agriculture, material science, and medical science communities (Elliott 1964; LeGeros et al. 1969; Regnier et al. 1994; Wilson et al. 1999; Suetsugu et al. 2000; Leventouri et al. 2000; Ivanova et al. 2001; Fleet and Liu 2004; Fleet et al. 2004; Wilson et al. 2004). The ideal structure of carbonate-free fluorapatite [$Ca_5(PO_4)_3F$] comprises of three types of cation polyhedra (i.e., the PO_4 tetrahedron, the $Ca1O_9$ polyhedron, and the $Ca2O_6F$ polyhedron), with the F atoms in the anion column parallel to the crystallographic c axis and three symmetry independent O atoms (labeled O1, O2, and O3; Hughes et al. 1989; Hughes and Rakovan 2002). Carbonate ions in apatites can substitute for F^- or OH^- in the anion column (Type A) and for the phosphate ion (Type B) (Elliott 1964; Gilinskaya et al. 1971; Regnier et al. 1994; Suetsugu et al. 2000; Ivanova et al. 2001; Fleet et al. 2004). Fleet and Liu (2004) and Fleet et al. (2004) reported results of a single-crystal X-ray structure and Fourier-transform infrared (FTIR) spectroscopic study of carbonate-rich apatites synthesized at high pressures and recognized one additional location for carbonate ions: i.e., a stuffed position in the anion column (Type A2) distinct from the regular anion column position (re-labeled as Type A1).

However, there remain considerable uncertainties and current debates about the structural environments of Type B carbonate ions (Elliott 1964; Regnier et al. 1994; Wilson et al. 1999, 2004; Suetsugu et al. 2000; Leventouri et al. 2000; Ivanova et al. 2001; Fleet and Liu 2004; Fleet et al. 2004). Most authors suggested that the carbonate ion lies on the sloping face of the PO_4^{3-} tetrahedron and hence is inclined with respect to the crystallographic c axis (Elliott 1964; Wilson et al. 1999, 2004; Fleet and Liu 2004; Fleet et al. 2004), although other orientations have been proposed (i.e., perpendicular to the c axis: Gilinskaya et al. 1971; Leventouri et al. 2000; parallel to the c axis: Ivanova et al. 2001). Also, charge compensation mechanisms for heterovalent substitution of CO_3^{2-} for PO_4^{3-} remain unclear (Regnier et al. 1994; Pan and Fleet 2002; Fleet and Liu 2004). For example, most earlier studies of carbonate-bearing fluorapatite and hydroxylapatite emphasized the presence of "excess" F and OH, and proposed the formation of $[CO_3F]^{3-}$ or $[CO_3OH]^{3-}$ for accommodating Type B carbonate ions. However, structural evidence for the presence of $[CO_3F]^{3-}$ or $[CO_3OH]^{3-}$ is lacking (Regnier et al. 1994; Pan and Fleet 2002). Fleet and Liu (2004) proposed several alternative options for charge balancing the partial substitution of PO_4^{3-} by CO_3^{2-} in apatites, including vacancies or Na at Ca positions, dehydroxylation of residual OH, and carbonate in the anion column.

As part of our continuing effort to better understand the anion column in the apatite-group minerals and related compounds (Nokhrin et al. 2005; Yang et al. 2005), we investigated carbonate-bearing fluorapatite by single-crystal electron paramagnetic

* E-mail: yuanming.pan@sask.usask.ca

0003-004X/06/0809–1425$05.00/DOI: 10.2138/am.2006.2142

resonance (EPR) spectroscopy. Results reported herein reveal three oxygen-associated hole-like defect centers and a CO_2^- radical in the anion column. One of these oxygen-associated hole-like defect centers is new to the apatite-group minerals and provides new insights into not only the orientation but also charge compensating mechanism of Type B carbonate ions in apatites. Although the CO_2^- radical has been previously studied in carbonate-bearing hydroxylapatite (Sadlo et al. 1998; Schramm et al. 2000; Vanhaelewyn et al. 2000), investigations of this radical in fluorapatite have not been reported.

Samples and experimental techniques

Three samples of carbonate-bearing fluorapatite (1: Levant mine, St. Just, Cornwall, England; 2: Perth, Ontario, Canada; and 3: Minas Gerais, Brazil; Yang et al. 2005) have been selected for this study. Fragments of each sample were mounted in a Pyrex plug and polished for electron microprobe analysis (EMPA) on a JEOL JXA-8600 Superprobe at the Department of Geological Sciences University of Saskatchewan. Operating conditions included an accelerating voltage of 15 kV, a beam current of 10 nA, beam diameter of 2 μm and counting times of 30 to 60 s, with the following mineral standards (quartz = Si; jadeite = Na and Al; fluorapatite = P and Ca; fluorite = F; Celestine = Sr; and tugtupite = Cl). Handpicked grains of carbonate-bearing fluorapatite were powdered for FTIR absorption spectroscopic and X-ray diffraction (XRD) analysis. FTIR spectra were collected on KBr pellets using the BIO-RAD FTS-40 spectrometer at the Saskatchewan Structural Science Centre, University of Saskatchewan. Powder XRD patterns in the 2θ range of 50–55° were collected on a Rigaku Rotaflex diffractometer, using Ni-filtered Cu$K\alpha$ radiation and a scan rate of 0.125° 2θ/min (cf. Schuffert et al. 1990).

The Levant carbonate-bearing fluorapatite crystals selected for the EPR spectroscopic study are brownish hexagonal plates, consisting of the basal plane and a prism, twinned in six triangular sectors. The brownish color is at least partly attributable to surface coating and inclusions of hematite. The triangular sectors extinguish at about 60° with respect to one another; some sectors may exhibit slightly undulatory extinction, but no appreciable departure from uniaxiality. The Perth carbonate-bearing fluorapatite crystals are light bluish in color, whereas those from Minas Gerais, Brazil are light pink to purplish in color. Procedures employed for single-crystal EPR experiments are similar for all three samples, and only those for the Levant crystals are described below.

A fragment of the Levant carbonate-bearing fluorapatite selected for X-band (~9.0 GHz) EPR measurements is approximately $3 \times 2 \times 0.8$ mm and consists of one large and three much smaller triangular sectors. This fragment was first examined on a Bruker ESP300E spectrometer and then irradiated at room temperature (RT) in a ^{60}Co cell at 0.37 Gray/s for 4 h, at the Department of Chemistry, University of Saskatchewan. EPR spectra of the gamma-irradiated carbonate-bearing fluorapatite were recorded at 77 K using an X-band spectrometer at the Illinois EPR Research Center (IERC), University of Illinois at Urbana-Champaign. Field-swept EPR spectra were measured at 15° intervals with the magnetic field B in three orthogonal rotation planes. Experimental uncertainty in angle measurement is approximately 0.5°. Following Chen et al. (2002a, 2002b), the rotational axes **z** and **y** of the experimental system are chosen along the crystallographic c and a axes, respectively, of the largest triangular sector on the twinned fragment, and axis **x** is defined as perpendicular to both **y** and **z**. Alignment of the twinned fragment was made approximately by use of the basal faces and a well-developed prismatic face of the largest triangular sector. The spectral resolution was approximately 0.02 mT (i.e., 2048 field data points over 40 mT in each spectrum) for all three rotation planes. Magnetic field calibration was made by use of 2,2-diphenyl-picrylhydrazyl (DPPH; g = 2.0037).

After the completion of X-band EPR measurements, the twinned fragment was broken apart to isolate a piece of the largest sector for W-band (~94 GHz) EPR experiments at 77 K. Single-crystal W-band EPR spectra for three orthogonal rotation planes, similar to those defined above, were obtained on a Mark II spectrometer at IERC. The B-field calibration of the W-band spectrometer was made by use of a Metrolab NMR Teslameter PT2025 (Nilges et al. 1999). The resolution of W-band spectra was 0.024 mT (i.e., 4096 field data points over 100 mT in each spectrum).

Another fragment of the Levant carbonate-bearing fluorapatite was first investigated by X-band EPR after gamma irradiation and then subjected to partial dissolution in dilute HF. The HF-treated fragment was then re-measured at RT on the Bruker X-band ESP300E spectrometer at the Department of Chemistry, University of Saskatchewan.

The calculations of spin Hamiltonian parameters, angle corrections for the Zeeman-field directions and simulations of X- and W-band EPR spectra were all performed using the software package EPR-NMR (Mombourquette et al. 1996).

Results

Sample characterization

Ten EMPA spot analyses of the Levant carbonate-bearing fluorapatite yielded an average (standard deviation in parenthesis) of 38.2(9) wt% P_2O_5, 57.6(7) CaO, 0.14(6) SrO, 0.08(3) BaO, 0(0) MnO, 0.03(4) FeO, 0.03(3) Na_2O, 4.63(5) F, and 0(0) Cl. The empirical equation of Schuffert et al. (1990), using a measured $\Delta 2\theta$ value between the 004 and 410 powder XRD reflections, gave a CO_2 content of 2.54 wt%. The presence of a significant amount of carbonate in the Levant fluorapatite is confirmed by well-resolved absorption peaks at ~865, 1426, and 1453 cm^{-1} in its FTIR spectrum (Fig. 1). These peaks in fluorapatite have been assigned to the ν_2 and ν_3 normal modes of Type B carbonate substituting for the PO_4^{3-} group (Elliott 1964; Regnier et al. 1994; Fleet et al. 2004 and references therein). In addition, spectral fitting suggests the possible presence of two low-intensity absorption bands at 1535 and 1458 cm^{-1}, corresponding to the ν_{3a} and ν_{3b} bands of Type A carbonate ion (Fig. 1b; Elliott 1964; Regnier et al. 1994; Fleet et al. 2004). The ratio between Types B and A carbonate ions in this sample, estimated on the basis of the band areas, is 15:1 (Fig. 1b).

EMPA analyses confirm that the Perth and Minas Gerais samples are also fluorapatite, and powder XRD yielded 0.25 and 0.11 wt% CO_2, respectively. The FTIR spectra also confirm that both types of carbonate ions are present and that Type B carbonate ion predominates over its Type A counterpart in these two samples as well (Fig. 1a).

X-band EPR spectra of the Levant carbonate-bearing fluorapatite

The X-band EPR spectrum of the Levant carbonate-bearing fluorapatite without gamma irradiation does not reveal any paramagnetic centers. However, the RT and 77 K X-band EPR spectra of this sample after gamma irradiation disclose several resonance absorption lines (Fig. 2). Careful analysis of their experimental roadmaps indicates at least four distinct paramagnetic centers: two electron-spin S = 1/2 centers of axial symmetry and two S = 1/2 orthorhombic centers (Fig. 2).

The EPR spectra of the first axial center, when the Zeeman magnetic field **B** is close to the c axis, consist of three lines with intensity ratio 1:2:1 (labeled HII in Fig. 2a; see below), indicative of hyperfine interaction with two equivalent nuclei of nuclear spin I = 1/2. When **B** is perpendicular to the c axis, however, the three lines converge into a single line (Fig. 2b).

The EPR spectra of the second axial center at **B** close to the c axis consist of two lines of equal intensity (labeled HI in Fig. 2a; see below), indicative of hyperfine interaction with one nucleus of I = 1/2. Similar to the first axial center, the two lines of the second axial center also converge into one when **B** is perpendicular to the c axis (Fig. 2b).

The 77 K X-band EPR spectra also disclose a center with g-factors close to that of a free electron (g_e = 2.0023 or magnetic field B at ~323.2 mT; labeled "CO_2^-" in Figure 2b). This center

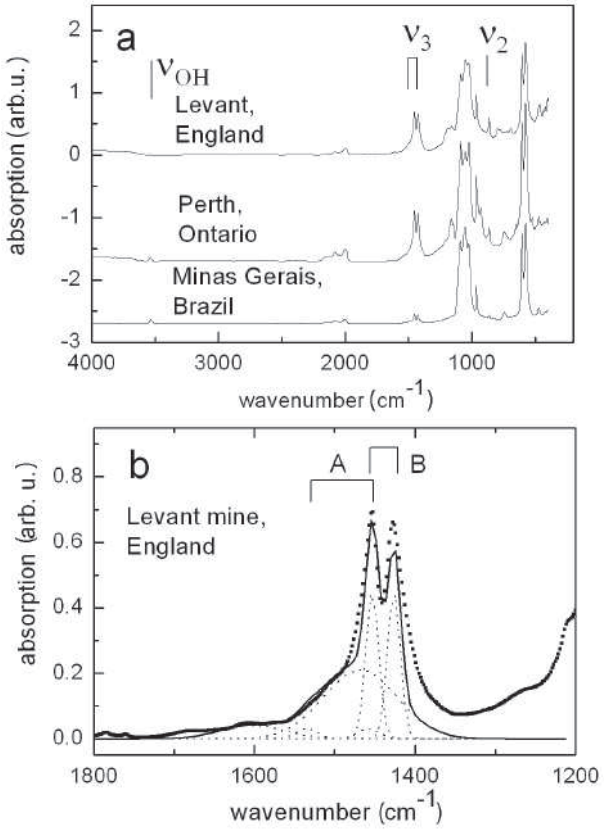

FIGURE 1. (**a**) FTIR spectra of carbonate-bearing fluorapatite from the Levant mine (Cornwall, England), Perth (Ontario, Canada), and Minas Gerais (Brazil); Note that the characteristic modes of Type B carbonate (ν_2 at 865 cm^{-1} and ν_3 at 1426 and 1453 cm^{-1}) and that of hydroxyl (ν_{OH} at 3537 cm^{-1}) are labeled. (**b**) Comparison of measured (heavy dotted line) and calculated (solid line) FTIR spectra of the Levant carbonate-bearing fluorapatite in the 1200–1800 cm^{-1} region. Spectral fitting included Gaussian distributions for bands (light dotted lines) related to stretching ν_3 of Type B and A carbonate ions; extra peaks were also added for better fitting.

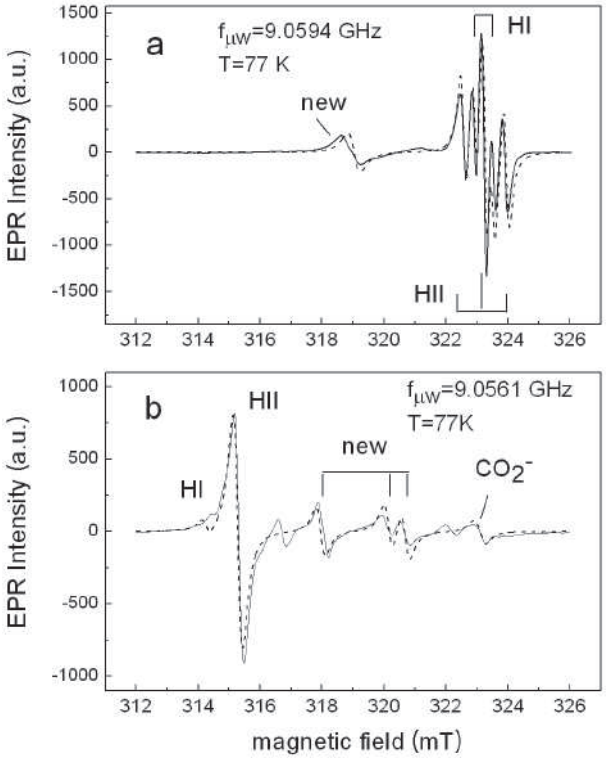

FIGURE 2. Single-crystal X-band EPR spectra of gamma-irradiated Levant carbonate-bearing fluorapatite at 77 K with Zeeman magnetic field orientation **B**: (**a**) parallel to the z axis and (**b**) parallel to the y axis. Dashed lines show simulated EPR spectra. Note that additional lines are present in **b** and may represent other paramagnetic defect centers. HI and HII denote the $O^-\square_F$ and O^- defects, respectively.

is also approximately axial, but its orthorhombic symmetry is indicated by splitting into 2 or 3 lines observed at several orientations (i.e., when **B** is inclined to the c axis), although these lines are not well resolved owing to significant linewidths. The intensity of this weakly orthorhombic center is much lower than those of all other centers (Fig. 2b).

The X-band EPR spectra also disclose a well-resolved orthorhombic hole-like center (labeled "new" in Fig. 2). The EPR spectra of this orthorhombic center are characterized by three lines in plane **xy** (Figs. 2b and 3c). However, six lines are well resolved in both **xz** and **yz** planes when B is away from the c axis (Figs. 3a and 3b). However, this six-line spectrum exhibits a sixfold symmetry about the crystal [0001] direction and collapses into a single resonance absorption line when **B** is parallel to the c axis (Figs. 2a, 3a, and 3b).

The X-band EPR spectra of this study were expected to be complicated by crystal twinning. However, resonance absorption lines expected from twinning (i.e., determined by spectral simulations) are not detected for any of the observed paramagnetic centers, including the strongly orthorhombic center. This apparent absence of twinning is probably attributable to the fact that the one triangular sector is significantly larger than the other three and, hence, resonance absorption lines from the three small sectors may not be detectable.

W-band EPR spectra of the Levant carbonate-bearing fluorapatite

The single-crystal W-band EPR spectra are invariably low in signal-to-noise ratios but do disclose the first of the axial hole-like center observed in the X-band spectra. However, the hyperfine splitting of this axial hole-like center was not resolved in the W-band spectra due to much larger linewidths. Also, the lines of the strongly orthorhombic center were observed at magnetic field orientations close to the c axis. It is noteworthy that no additional paramagnetic centers are observed in the W-band spectra. The large linewidths and poor signal-to-noise ratios of the W-band EPR spectra are presumably due to inhomogeneous line broadening and/or longer spin-lattice relaxation time. Another potential factor is inappropriate crystal size (too large), which may result in a low effective unloaded quality factor (Q) of the resonant cavity and difficulty in tuning. Therefore, all data analyses and interpretation in this study are based on the X-band spectra.

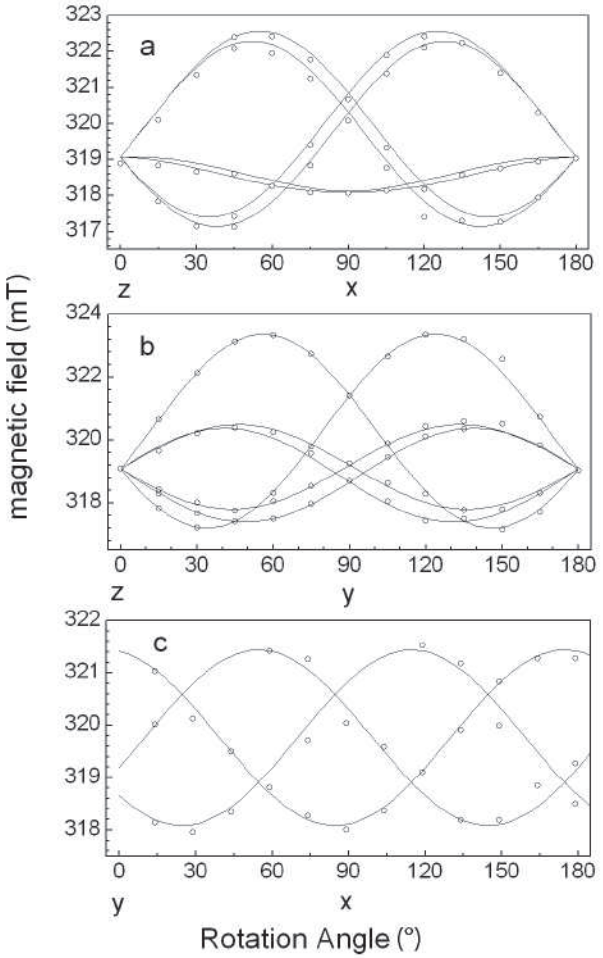

FIGURE 3. Angular dependence of X-band EPR spectra of the new hole-like defect center in gamma irradiated Levant carbonate-bearing fluorapatite at 77 K with the Zeeman magnetic field **B** in (**a**) the **yz** plane, (**b**) the **xz** plane, and (**c**) the **xy** plane. Open circles represent the observed data points; solid lines computed with the optimized spin Hamiltonian parameters (Table 1).

X-band EPR spectra of HF-treated Levant carbonate-bearing fluorapatite

Several radiation-induced paramagnetic defects have been reported to occur on the surfaces of synthetic carbonate-bearing fluorapatite (Elliott 1994 and references therein). Accordingly, X-band EPR measurements were made on a gamma-irradiated sample before and after immersion in dilute HF to determine whether the paramagnetic centers observed in this study are surface defects. The RT X-band EPR spectra of HF-treated carbonate-bearing fluorapatite show the presence of all four defects described above, except that the weakly orthorhombic center observed at 77 K is now axial in symmetry (see below). We conclude, therefore, that all defects observed in this study are of bulk nature and are not restricted to the crystal surfaces.

X-band EPR spectra of Perth and Minas Gerais carbonate-bearing fluorapatite

The single-crystal EPR spectra of gamma-irradiated carbonate-bearing fluorapatite from Perth, Ontario are similar to those of the Levant sample and reveal the presence of the same four paramagnetic centers. The EPR spectra of carbonate-bearing fluorapatite from Minas Gerais, Brazil, however, are characterized by high-intensity and very broad lines corresponding to the $^{55}Mn^{2+}$ center at the Ca1 site (Pan et al. 2002 and references therein). The presence of this Mn center precludes observation of any other paramagnetic centers with g values close to 2.0 in this sample.

DISCUSSION

The spin Hamiltonian used in interpreting the EPR spectra of this study takes the form:

$$H = g_x\beta B_x S_x + g_y\beta B_y S_y + g_z\beta B_z S_z + \Sigma_i (A^i_x S_x I^i_x + A^i_y S_y I^i_y + A^i_z S_z I^i_z) \quad (1)$$

where β is the Bohr magneton and $g_{x,y,z}$ and $A_{x,y,z}$ are the principal values of the g-factor values and hyperfine splitting parameters, respectively.

The X-band EPR spectra of gamma-irradiated carbonate-bearing fluorapatite crystal from the Levant mine, England and Perth, Ontario disclose four paramagnetic centers. The two axial centers correspond to two oxygen hole centers previously reported in fluorapatite (see below). The spin Hamiltonian parameters of these two centers were obtained by (1) spectral simulations using previously reported spin Hamiltonian parameters (Piper et al. 1965); (2) comparison of calculated roadmaps and experimental roadmaps; and (3) modification of the previously reported spin Hamiltonian parameters to best fit the observed EPR spectra and roadmaps.

The center of weakly orthorhombic symmetry at 77 K and axial symmetry at RT corresponds to a CO_2^- radical previously reported in carbonate-bearing hydroxylapatite (see below). The optimization of the spin Hamiltonian parameters of this center, using the software package EPR-NMR, was performed for the 77 K and the RT spectra, separately, owing to their difference in symmetry. At both temperatures, spin Hamiltonian optimization was commenced with $A_x = A_y = A_z = 0$ mT because no hyperfine interaction was observed. The final root-mean-sum-of-squares of weighted differences (RMSD) between the calculated and observed line positions at RT is 0.023 mT, which is less than the half width of the observed absorption lines (0.21 mT). The final RMSD between the calculated and observed line positions at 77 K is 0.041 mT. The larger RMSD value at 77 K is partly attributable to the poorly resolved site splitting of this center at this temperature.

The strongly orthorhombic center is a new paramagnetic defect in apatite-group minerals. The spin Hamiltonian parameters of this center were obtained by fitting of all experimental line-position data from three orthogonal rotation planes, using the software package EPR-NMR. Spin Hamiltonian optimization of this new center was also commenced with $A_x = A_y = A_z = 0$ mT because no hyperfine interaction was observed. The final RMSD for this center is 0.06 mT, which is much less than the half width of absorption lines (0.2 mT).

HII center

The EPR spectra of the first axial center, characterized by hyperfine interactions with two equivalent nuclei of I = 1/2, are

similar to those of the O^- defect center in the anion column of fluorapatite, which has been previously identified and characterized by Segall et al. (1962) and Piper et al. (1965). This interpretation is confirmed by the calculated spin Hamiltonian parameters ($g_x = g_y = 2.0522$, $g_z = 2.0018$; $A_x/g_e\beta_e = A_y/g_e\beta_e = 0.032$ mT, $A_z/g_e\beta_e = 0.695$ mT). This center is due to a hole trapped by an isolated O^{2-} ion substituting for an F^- ion after ionizing irradiation. Since the O^- ion is located between two fluorine ions the unpaired electron interacts with two equivalent fluorine nuclei (I = 1/2), giving rise to the observed hyperfine structure (Fig. 2a). Segall et al. (1962) showed that in this O^- center the unpaired electron occupies the $\sigma(p_z)$ orbitals and that the $\pi(p_x, p_y)$ energy levels are lower than the $\sigma(p_z)$ level as seen from consideration of the crystal field of the nearest neighbors, which are three Ca^{2+} ions positioned in the mirror plane perpendicular to the c axis. In this structural model the observed g-factor values can be explained, and the c axis must be the axis of symmetry of this center. Also, the weak hyperfine splitting from interaction with two fluorine nuclei and its anisotropy are explained by this model, by calculation of the expected ^{19}F hyperfine interaction parameters, based on the Hartree-Fock radial wave functions for the O^- and F^- orbitals. Piper et al. (1965) further confirmed this structural model by use of ^{19}F and ^{31}P electron nuclear double resonance (ENDOR) measurements and named it the HII center.

HI center

The X-band EPR spectra of the second axial center are similar to the previously reported HI center in fluorapatite (Piper et al. 1965). This similarity is confirmed by the calculated spin Hamiltonian parameters ($g_x = g_y = 2.0582$, $g_z = 2.0019$; $A_x/g_e\beta_e = A_y/g_e\beta_e = 0.021$ mT, $A_z/g_e\beta_e = 0.577$ mT). This center has been interpreted to arise from a hole trapped by an O^{2-} ion situated at an F^- site next to an F^- vacancy (i.e., an $O^-\square_F$ configuration, where $\square_F$ represents a vacancy in the F site) in the anion column. In this configuration, the unpaired electron interacts with only one fluorine nucleus and, hence, the observed hyperfine structure (Fig. 2a).

Piper et al. (1965) noted that this center in synthetic fluorapatite was observed only at temperatures below 225 K and after X-ray irradiation at liquid nitrogen temperature. At temperatures near 225 K, the HI center first decreases in intensity and then disappears completely, whereas the intensity of the HII center increases proportionally. Piper et al. (1965) noted that the $O^{2-}\square_F$ defect is electrically neutral and, therefore, may capture a positively charged hole under ionizing irradiation. However, after the formation of the O^- ion by trapping a hole, the vacancy may be easily pulled away, thus converting the $O^-\square_F$ defect center to the O^- defect (i.e., the HII center). Our detection of the HI center at RT suggests that fluorine vacancies may be less mobile in natural carbonate-bearing fluorapatite. It is possible that this $O^-\square_F$ defect in natural carbonate-bearing fluorapatite is stabilized by other defects such as Ca vacancies and/or substitution defects at the $(PO_4)^{3-}$ site (e.g., Type B carbonate ion; see below).

CO_2^- radical

The calculated spin Hamiltonian parameters of the electron-like center in carbonate-bearing fluorapatite at 77 K and RT (Table 1) match closely to those for the CO_2^- radical in hydroxylapatite at those temperatures (Sadlo et al. 1998; Schramm et al. 2000; Vanhaelewyn et al. 2000). Similarly, Schramm et al. (2000) noted that the powder EPR spectra of the CO_2^- radical in hydroxylapatite measured at low temperature are of orthorhombic symmetry, but become axial in symmetry at RT. The single-crystal EPR study by Vanhaelewyn et al. (2000) confirmed that the CO_2^- radical in hydroxylapatite at RT is of axial symmetry. The orthorhombic symmetry of the CO_2^- radical in calcite has been demonstrated by single-crystal EPR studies at 77 K (Marshall et al. 1964). Marshall et al. (1964) reported the principal values $g_{z'} = 2.0016$, $g_{x'} = 2.0032$, and $g_{y'} = 1.9972$ for the CO_2^- radical in calcite, where the coordinate system (x′, y′, and z′) is referenced to the CO_2^- molecule-ion. These authors also noted that $g_{y'}$ of this radical is parallel to the O-O direction, whereas $g_{z'}$ is parallel to the direction of the bisector of the O-C-O angle and $g_{x'}$ is perpendicular to the O-C-O plane. Schramm et al. (2000) attributed the axial symmetry of the CO_2^- radical in hydroxylapatite at RT to the rotation of this radical about the O-O direction (see also Vanhaelewyn et al. 2000). However, Vanhaelewyn et al. (2000) proposed the possible presence of two CO_2^- radicals with slightly different spin Hamiltonian parameters to account for their observed line broadening at 90 K. On the basis of our observed line splitings at 77 K and the symmetry of this radical in calcite (Marshall et al. 1964), we favor a symmetry reduction from RT to 77 K (Table 1). Schramm et al. (2000), on the basis of their ENDOR study and electronic structural calculations, also suggested that the CO_2^- radical in carbonate-bearing hydroxylapatite resides in the anion column and is located between the two oxygen planes (z = 0.426 and 0.574). Similarly, the orientation of the CO_2^- radical in carbonate-bearing fluorapatite suggests that this radical most likely resides in the anion column and probably formed from Type A carbonate ions by the loss of an O atom and trapping of an electron during gamma irradiation. Also, the recognition of this CO_2^- radical in the Levant and Perth carbonate-bearing fluorapatite is supported by FTIR data for the presence of Type A carbonate ions in these samples (Fig. 1).

The unique symmetry axis of the CO_2^- radical in carbonate-bearing fluorapatite at both 77 K and RT is approximately

TABLE 1. Spin Hamiltonian parameters of the CO_2^- radical at 77 K and room temperature and the new orthorhombic O^- center at 77 K in carbonate-bearing fluorapatite

g-matrix			K	Principal values g_k	Principal directions	
					θ_k	φ_k
CO_2^- radical, 77 K						
2.0028(2)	−0.00071(1)	0.0003(1)	1	2.0033(2)	88(2)	326(5)
	2.0023(2)	0.00000	2	2.0018(2)	88(2)	56(5)
		1.9968(1)	3	1.9968(1)	3(1)	187(5)
CO_2^- radical, room temperature						
2.00240(7)	0.00000	0.0000	1	2.00240(7)	90(2)	0(2)
	2.00240(7)	0.0000	2	2.00240(7)	90(2)	90(2)
		1.9968(1)	3	1.9968(1)	0(2)	0(2)
new O^- center, 77 K						
2.01397(2)	0.00196(2)	−0.01802(2)	1	2.0412(1)	143.0(4)	23.0(1)
	2.03493(2)	−0.00050(2)	2	2.0346(2)	77(1)	96.0(6)
		2.02873(2)	3	2.0018(1)	56.0(1)	357.0(3)

Note: g matrices reported herein are referenced to the symmetry of the host crystal (see text for definition), different from the conventional notation for the CO_2^- radical with respect to its molecular coordinate system (e.g., Marshall et al. 1964).

parallel to the crystallographic c-axis (Table 1), suggesting that its O-O direction is approximately "vertical." In this configuration, superhyperfine interaction with ^{19}F nuclei is not expected because the unpaired electron in the CO_2^- radical occupies the $3a_1$* antibonding orbital formed mainly from the carbon s and p_z orbitals (Marfunin 1979) and is well separated from those nuclei. The orientation of the CO_2^- radical in carbonate-bearing fluorapatite from our single-crystal EPR spectra is similar to that in hydroxylapatite from the single-crystal study of Vanhaelewyn et al. (2000), but notably different from that reported by Schramm et al. (2000) who suggested that the angle between the radical O-O direction and the c axis is ~26° in hydroxylapatite. However, the powder experiments of Schramm et al. (2000) may contain larger uncertainties on orientation than single-crystal measurements. It is noteworthy that polarized IR experiments suggested that the angle between the plane of the carbonate ion CO_3^{2-} (i.e., the precursor of the CO_2^- radical) and the c axis is <27° (Elliott 1994). Single-crystal X-ray diffraction studies of carbonate hydroxylapatite (Fleet and Liu 2004; Fleet et al. 2004) showed that the carbonate ion substituting two OH^- is ordered along the anion column at z = 0.5 and oriented with two of its O atoms close to the c-axis (i.e., the CO_3 plane was found to be tilted from the vertical by approximately 12°).

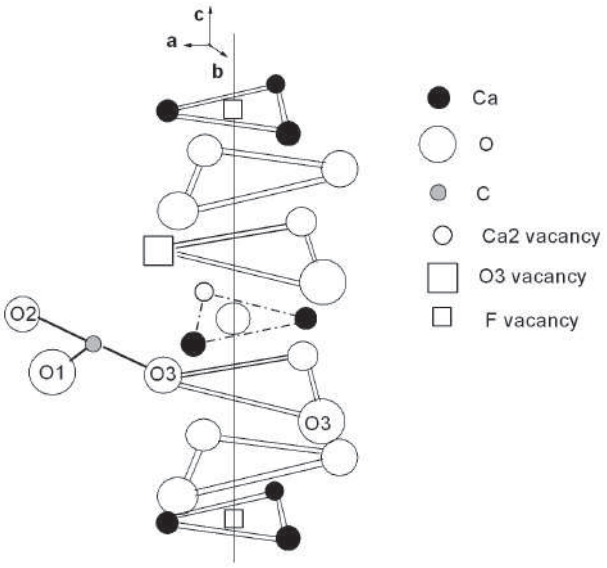

FIGURE 4. Structural model for the new oxygen-associated hole-like center in carbonate-bearing fluorapatite (for the positions of the P, Ca1, Ca2, O1, O2, O3, and F atoms in the ideal fluorapatite structure, see Hughes et al. 1989; Hughes and Rakovan 2002).

New hole-like center

The spin Hamiltonian parameters of the new orthorhombic center are given in the Table 1. The principal g-matrix values of this center are similar to those for the two oxygen-associated hole-like centers (i.e., HI and HII) in the anion column. Therefore, this new center may also represent an oxygen-associated hole-like O^- center in the anion column. The absence of any hyperfine splitting from ^{19}F nuclei suggests that the O^- ion is sandwiched between two fluorine vacancies. The $\square_F O^{2-} \square_F$ configuration has been reported as the precursor to the EI center in fluorapatite (Piper et al. 1965). The $\square_F O^{2-} \square_F$ defect has one positive charge (relative to the ideal $F^- F^- F^-$ configuration) and therefore is able to trap an electron to form the electron-like EI center, which is of an axial symmetry (Piper et al. 1965). The strong orthorhombic nature of the new oxygen-associated hole-like center suggests that the $\square_F O^{2-} \square_F$ configuration is disturbed by neighboring substitutions (e.g., vacancy at the neighboring Ca2 site; Fig. 4). Moreover, the exclusive occurrence of this new center in carbonate-bearing fluorapatite (and its presence in both Levant and Perth carbonate-bearing fluorapatite) suggests that it is most likely related to Type B carbonate ions through a complex substitution of the type: $\square_F O^{2-} \square_F + \square_{Ca2} + CO_3^{2-} = F \cdot F \cdot F^- + Ca^{2+} + PO_4^{3-}$. The $\square_F O^{2-} \square_F + \square_{Ca2} + CO_3^{2-}$ configuration is electrostatically neutral and therefore is capable of trapping a positively charged hole at the substitutional oxygen ion in the anion column. The orientation of the principal symmetry axis of the g matrix (see Table 1) suggests that disturbance comes from vacancies at both the neighboring Ca2 and O3 sites (Fig. 4; cf. Hughes et al. 1989; Hughes and Rakovan 2002). It is possible, therefore, that Type B carbonate ions associated with vacancies at the neighboring Ca2 site may form from a missing O3 and hence lie on the slope face of the PO_4^{3-} group (i.e., Elliott 1964; Wilson et al. 1999, 2004; Fleet and Liu 2004; Fleet et al. 2004).

The proposed structural model for this new center (Fig. 4) is further supported by its similarity in the g-matrix to well-studied O^- defect centers with neighboring-cation vacancies in alkali earth oxides (Henderson and Wertz 1977 and references therein). This type of O^- defect centers in alkali earth oxides has been shown to have the unpaired electron on the p_z-orbital oriented toward the positive cation vacancy, resulting in a g matrix that has one of its principal values very close to that of a free electron ($g_3 \sim g_e$) and the other two values are significantly larger ($g_1 > g_2 > g_e$; see Table 1). Moreover, the absence of hyperfine interaction with ^{31}P nucleus (I = 1/2, natural abundance = 100%) suggests that this new center in carbonate-bearing fluorapatite is not related to the various PO_3^{2-}-related radicals in apatites, which are known to have different spin Hamiltonian parameters (Shcherbakova et al. 1970; Gilinskaya 1990).

Finally, Gilinskaya et al. (1971) reported powder EPR spectra of two carbonate radicals (CO_3^- and CO_3^{3-}) in carbonate-bearing fluorapatite and interpreted those radicals to have formed from the loss and gain of an electron from Type B carbonate ions, respectively. Unfortunately, Gilinskaya et al. (1971) did not specify whether they irradiated their carbonate-bearing fluorapatite samples. These carbonate radicals are not evident in our crystals of carbonate-bearing fluorapatite before and after gamma irradiation. Nevertheless, the powder EPR spectra of these carbonate radicals (Gilinskaya et al. 1971) do not show any evidence of superhyperfine interaction from ^{19}F nuclei, supporting accumulating evidence that $[CO_3F]^{3-}$ does not appear to be present in carbonate-bearing fluorapatite (Regnier et al. 1994; Pan and Fleet 2002, references therein).

ACKNOWLEDGMENTS

We thank three referees and B. Wopenka for constructive reviews and helpful suggestions, M.E. Fleet for discussions and suggestions on the orientation of Type B carbonate ions, T. Bonli (EMPA and powder XRD), and K. Thomas (FTIR) for

analytical assistance, and the Natural Science and Engineering Research Council (NSERC) of Canada for financial support.

REFERENCES CITED

Chen, N., Pan, Y., and Weil, J.A. (2002a) Electron paramagnetic resonance spectroscopic study of synthetic fluorapatite: Part I. Local structural environment and substitution mechanism of Gd^{3+} at the Ca2 site. American Mineralogist, 87, 37–46.

Chen, N., Pan, Y., Weil, J.A., and Nilges, M.J. (2002b) Electron paramagnetic resonance spectroscopic study of synthetic fluorapatite. Part II. Gd^{3+} at the Ca1 site, with a neighboring Ca2 vacancy. American Mineralogist, 87, 47–55.

Elliott, J.C. (1964) The crystallographic structure of dental enamel, related apatites. PhD thesis, University of London.

——— (1994) Structure and chemistry of the apatites and other calcium orthophosphates. Studies in Inorganic Chemistry. Elsevier, Amsterdam.

Fleet, M.E. and Liu, X. (2004) Location of type B carbonate ion in type A-B carbonate apatite synthesized at high pressure. Journal of Solid State Chemistry, 177, 3174–3182.

Fleet, M.E., Liu, X., and King, P.L. (2004) Accommodation of the carbonate ion in apatite: An FTIR and X-ray structure study of crystals synthesized at 2.4 GPa. American Mineralogist, 89, 1422–1432.

Gilinskaya, L.G. (1990) A new variety of PO_3^{2-}-center in apatite. Journal of Structural Chemistry, 31, 51–58 (in Russian).

Gilinskaya, L.G., Shcherbakova, M.Ya., and Zanin, Yu.N. (1971) Carbon in the structure of apatite according to electron paramagnetic resonance data. Soviet Physics—Crystallography, 15, 1016–1019.

Henderson, B. and Wertz, J.E. (1977) Defects in the alkaline earth oxides: with applications to radiation damage and catalysis, 159 p. Taylor and Francis, London.

Hughes, J.M. and Rakovan, J. (2002) The crystal structure of apatite, $Ca_5(PO_4)_3(F,OH,Cl)$. In M.J. Kohn, J. Rakovan, and J.M. Hughes, Eds., Phosphates, 48, p. 1–12. Reviews in Mineralogy and Geochemistry, Mineralogical Society of America, Chantilly, Virginia.

Hughes, J.M., Cameron, M., and Crowley, K.D. (1989) Structural variations in natural F, OH, and Cl apatites. American Mineralogist, 74, 870–876.

Ivanova, T.I., Frank-Kamenetskaya, O.V., Kol'tsov, A.B., and Ugolkov, V.L. (2001) Crystal structure of calcium deficient carbonated hydroxyapatite. Journal of Solid State Chemistry, 160, 340–349.

LeGeros, R.Z., Trautz, O.R., LeGeros, J.P., and Klein, E. (1969) Carbonate substitution in the apatite structure. Bulletin de la Societe Chimique de France, 1712–1728.

Leventouri, T.H., Chakoumakos, B.C., Moghaddam, H.Y., and Perdikatsis, V. (2000) Powder neutron diffraction studies of a carbonate apatite. Journal of Material Research, 15, 511–517.

Marfunin, A.S. (1979) Spectroscopy, luminescence, and radiation centers in minerals, 352 p. Springer Verlag, Berlin.

Marshall, S.A., Reinberg, A.R., Serway, R.A., and Hodges, J.A. (1964) Electron spin resonance absorption spectrum of CO_2^- molecule-ions in single crystal calcite. Molecular Physics, 8, 225–231.

Mombourquette, M.J., Weil, J.A., and McGavin, D.G. (1996) EPR-NMR User's Manual. Department of Chemistry, University of Saskatchewan, Saskatoon, Canada.

Nilges, M.J., Smirnov, A.I., Clarkson, R.B., and Belford, R.L. (1999) Electron paramagnetic resonance W-band spectrometer with a low-noise amplifier. Applied Magnetic Resonance, 16, 167–183.

Nokhrin, S., Pan, Y., Weil, J.A., and Nilges, M.J. (2005) Multifrequency EPR study of radiation-induced defects in chlorapatite. Canadian Mineralogist, 43, 1581–1588.

Pan, Y. and Fleet, M.E. (2002) Compositions of the apatite-group minerals: substitution mechanisms and controlling factors. In M.J. Kohn, J. Rakovan, and J.M. Hughes, Eds., Phosphates, 48, p. 13–39. Reviews in Mineralogy and Geochemistry, Mineralogical Society of America, Chantilly, Virginia.

Pan, Y., Chen, N., Weil, J.A., and Nilges, M.J. (2002) Electron paramagnetic resonance spectroscopic study of synthetic fluorapatite: Part III. Structural characterization of sub-ppm-level Gd and Mn in minerals at W-band frequency. American Mineralogist, 87, 1333–1341.

Piper, W.W., Kravitz, L.C., and Swank, R.K. (1965) Axially symmetric paramagnetic color centers in fluorapatite. Physical Review, 138, A1802–1804.

Regnier, P., Lasaga, A.C., Berner, R.A., Han, O.H., and Zilm, K.W. (1994) Mechanism of CO_3^{2-} substitution in carbonate-fluorapatite: Evidence from FTIR spectroscopy, ^{13}C NMR and quantum mechanical calculations. American Mineralogist, 79, 809–818.

Sadlo, J., Matthys, P., Vanhaelewyn, G., Callens, F., Mihalik, J., and Stachowicz, W. (1998) EPR and ENDOR of radiation-induced CO_{3D}^{3-} radicals in human tooth enamel heated at 400 °C. Journal of Chemical Society, Faraday Transaction 94, 3275–3278.

Schramm, D.U., Terra, J., Rossi, A.M., and Ellis, D.E. (2000) Configuration of CO_2^- radicals in γ-irradiated A-type carbonated apatites: Theory and experimental EPR and ENDOR studies. Physical Review B, 63, 024107-1–024107-14.

Schuffert, J.D., Kastner, M., Emanuele, G., and Jahnke, R.A. (1990) Carbonate-ion substitution in francolite: A new equation. Geochimica et Cosmochimica Acta 54, 2323–2328.

Segall, B., Ludwig, G.W., Woodbury, H.H., and Johnson, P.D. (1962) Electron spin resonance of a center in calcium fluorapatite. Physical Review, 128, 76–79.

Shcherbakova, M.Ya., Gilinskaya, L.G., and Zhidomirov, G.M. (1970) Paramagnetic defect centers of PO_3^{2-} in apatite. Str. Mol. Kvantovaya Khim., 69–70 (in Russian).

Suetsugu, Y., Takahashi, Y., Okamura, F.P., and Tanaka, J. (2000) Structure analysis of A-type carbonate apatite by a single-crystal X-ray diffraction method. Journal of Solid State Chemistry, 155, 292–297.

Vanhaelewyn, G.C.A.M., Morent, R.A., Callens, F.J., and Matthys, P.F.A.E. (2000) X- and Q-band electron paramagnetic resonance of CO_2^- in hydroxyapatite single crystals. Radiation Research, 154, 467–472.

Wilson, R.M., Elliott, J.C., and Dowker, S.E.P. (1999) Rietveld refinement of the crystallographic structure of human dental enamel. American Mineralogist, 84, 1406–1414.

Wilson, R.M., Elliott, J.C., Dowker, S.E.P., and Smith, R.I. (2004) Rietveld structure refinement of precipitated carbonate apatite using neutron diffraction data. Biomaterials, 25, 2205–2213.

Yang, K., Aguiar, P.M., Kroeker, S., and Pan, Y. (2005) Characterization of fluorine environments in fluorapatites. 88th Canadian Chemical Conference Abstracts. Saskatoon, Canada.

MANUSCRIPT RECEIVED NOVEMBER 9, 2005
MANUSCRIPT ACCEPTED APRIL 30, 2006
MANUSCRIPT HANDLED BY BRIGITTE WOPENKA